Intermediate velocity source of intermediate-mass fragments in the $^{40}Ca+^{40}Ca$ reaction at $E_{lab}=35$ MeV/nucleon

P. Pawłowski,[1] J. Brzychczyk,[1] A. J. Cole,[2] P. Désesquelles,[2] W. Gawlikowicz,[1] K. Grotowski,[1,4] P. Hachaj,[1] S. Micek,[1] R. Płaneta,[1] Z. Sosin,[1] A. Wieloch,[1] D. Benchekroun,[3] E. Bisquer,[3] A. Chabane,[2] A. Demeyer,[3] M. Charvet,[2] B. Cheynis,[3] E. Gerlic,[3] A. Giorni,[2] D. Guinet,[3] D. Heuer,[2] P. Lautesse,[3] L. Lebreton,[3] A. Lléres,[2] M. Stern,[3] L. Vagneron,[3] and J. B. Viano[2]

[1]*M. Smoluchowski Institute of Physics, Jagellonian University, Reymonta 4, 30-059 Cracow, Poland*

[2]*Institut des Sciences Nucléaires de Grenoble, IN2P3-CNRS/Université Joseph Fourier 53, Avenue des Martyrs, F-38026 Grenoble, Cedex, France*

[3]*Institut de Physique Nucléaire de Lyon, IN2P3-CNRS/Université Claude Bernard 43, Boulevard du 11 Novembre 1918, F-69622 Villeurbanne Cedex, France*

[4]*H. Niewodniczański Institute of Nuclear Physics, Radzikowskiego 152, 31-342 Cracow, Poland*

(Received 1 April 1997; revised manuscript received 2 December 1997)

Events with 3–5 intermediate mass fragments [(IMF's), $Z>2$] have been studied for peripheral and more central collisions in the $^{40}Ca+^{40}Ca$ reaction at $E_{lab}=35$ MeV/nucleon. For a significant portion of events, in coincidence with projectilelike and with targetlike fragments, we observe IMF's, with velocities close to zero in the center-of-mass reference frame. Properties of this ''intermediate velocity'' source suggest a stochastic character of its creation. Microscopic model calculations are also presented. [S0556-2813(98)02804-0]

PACS number(s): 25.70.Pq, 24.10.Nz, 25.70.Gh, 25.70.Lm

I. INTRODUCTION

The dynamics of peripheral heavy ion collisions exhibits a predominantly binary evolution characterized by strong energy dissipation at least at low collision energies (below about 10 MeV/nucleon) and large impact parameters [1]. Thus, in the exit channel, we observe targetlike and projectilelike fragments (TLF's and PLF's) which summed kinetic energy is much smaller than the entrance channel energy. For more central collisions the colliding ions form a compound nucleus which appears in the laboratory frame of reference as a single source moving with the center-of-mass (c.m.) velocity. At higher energies, above 10 to 20 MeV/nucleon, new phenomena appear, including significant preequilibrium emission, production of IMF's, projectile and target fragmentation, and incomplete fusion. Nevertheless collisions in this energy range are still reminiscent of binary dissipative processes [2]. At much higher energies the fusion cross section becomes negligible and the participant-spectator picture dominates [3].

Recently, a source of IMF's has been observed which is located between the velocities of PLF's and TLF's [the intermediate velocity source (IVS)] [4–6]. Such a source has been previously suggested at intermediate impact parameters (b) by Boltzmann-Uehling-Uhlenbeck (BUU) [7] and Boltzmann-Nordheim-Vlasov (BNV) [8] calculations. It was interpreted as a new type of neck instability coupled to dynamic fluctuations which increase with energy [8]. The mechanism could be similar to the multiple neck rupture in fission [9]. On the other hand, it cannot be exactly that of low-energy ternary fission where, e.g., an α particle is emitted in the scission configuration [10] because of the involved time scale [5]. It may be intermediate between the low-energy neck formation and the (high-energy) participant-spectator mechanism.

In this work we report on the observation of the IVS in the $^{40}Ca+^{40}Ca$ reaction at $E_{lab}=35$ MeV/nucleon. Globally, the source is observed in about 15% of all well-defined events and contains about 0.2 to 0.4 of the total charge.

The experimental data are presented in Sec. II. After briefly describing the experiment (Sec. II A), we discuss, successively, selection of impact parameters (Sec. II B), Galilean invariant (GI) velocity plots (Sec. II C), and charge (Z) distributions (Sec. II D). Transition towards more central collisions is discussed in Sec. II E.

In Sec. III we display and discuss results of microscopic BNV simulations. The results of these calculations are in qualitative agreement with our observations but significantly underestimate the importance of the intermediate velocity source. Summary and conclusions are given in Sec. IV.

II. EXPERIMENT

A. Experimental setup and data

The experiment was performed at the Grenoble SARA facility using the 4π multidetector system AMPHORA [11]. Additional 30 ionization chambers were installed on two AMPHORA rings at 31.2 ± 6.5 and 46.7 ± 8.9 degrees [12]. Their purpose was to lower energy thresholds for IMF's from 5–9 MeV/nucleon (standard AMPHORA) to about 1 MeV/nucleon. Without ionization chambers observation of the TLF source would not be possible. The global solid angle coverage was approximately 80%. Experimental details, and procedures are described in Refs. [13] and [14].

Distribution of the total charge detected by AMPHORA is broad with a mean value 22.3 (Fig. 1). However, as in [14] we impose the condition that for well defined events, used in further analysis, the total detected charge $Z_{tot}>30$. In the majority of events 2 IMF's are emitted but emission of 1, 3, 4, and 5 IMF's is also observed with reasonable statistics (see Fig. 2).

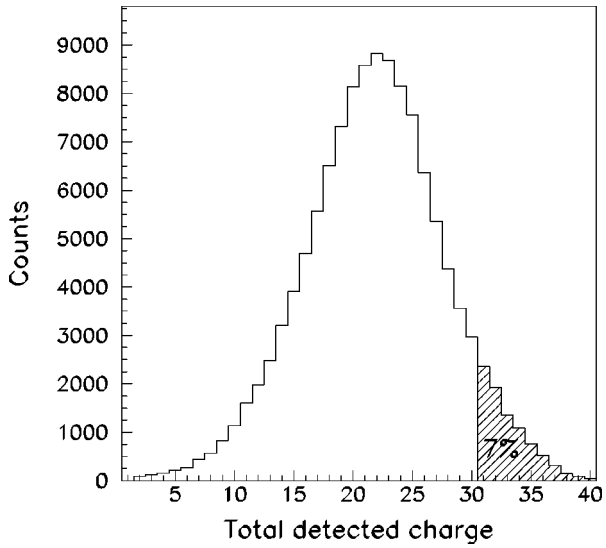

FIG. 1. Distribution of the total collected charge.

In our quest for the *IV* source we shall follow evolution of GI velocity distributions in different regions of b, due to suggestions [4–8] that it should be located at intermediate impact parameters.

B. Selection of impact parameters

We have shown in Ref. [14] that, in the case of our reaction, the angular momentum L versus charged particle multiplicity M dependence, although monotonic in average values, is very broad and saturates at lower L values. Therefore it cannot be used as a good impact parameter filter for more central collisions. It is, however, adequate for selecting collisions with average b values from 4 to 6 fm which we shall call midcentral collisions. Such b values correspond roughly to $100\hbar \leqslant L \leqslant 150\hbar$ and the range $5 \leqslant M \leqslant 13$ (see Fig. 7(a) in Ref. [14]).

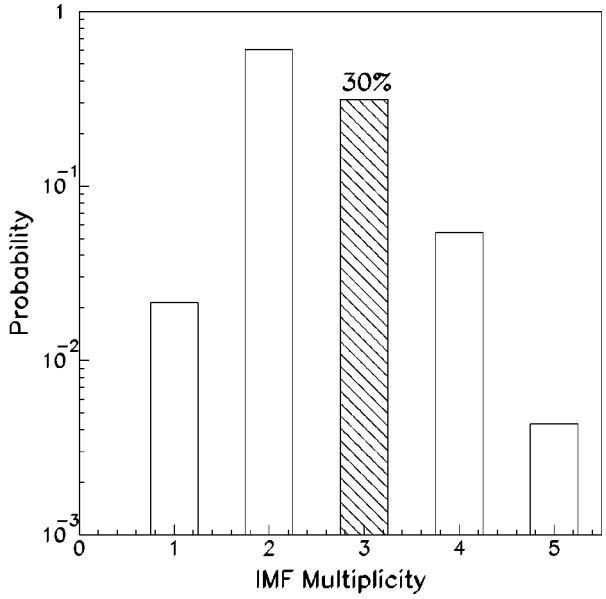

FIG. 2. Distribution of IMF multiplicity m for well defined events.

To select midcentral collisions we also employ as filters global variables η and ξ:

$$\eta = \frac{\Sigma_{i=1}^{m} E_i}{\Sigma_{i=1}^{m} A_i}, \tag{1}$$

$$\xi = \frac{\Sigma_{i=1}^{M} Z_i^2}{\Sigma_{i=1}^{M} Z_i}, \tag{2}$$

where m denotes IMF multiplicity and E_i, A_i, and Z_i is the c.m. energy, mass number, and atomic number of the ith IMF in the event, respectively. The heaviest IMF is omitted in Eq. (2). This quantity ($\xi = S_2$) was used originally by Campi [15] to study fluctuations in fragment sizes. For our reaction it is used to select midcentral collisions. We use here, 2 MeV/nucleon $< \eta <$ 6 MeV/nucleon, and $0.5 < \ln\xi < 2$. As checked by simulations, quantities η, and $\ln\xi$ are large for peripheral collisions and small for more central ones (see also [16]).

These three filters select a similar region of b, but because of some correlations, probably not exactly the same sets of events.

C. Different sources of IMF's

Figure 3 presents invariant velocity plots for IMF's emitted in different bins of the impact parameter, which are selected with three different filters: M, η, and $\ln(\xi)$. The figure was prepared using events with three emitted IMF's. It shows evolution from two IMF sources for most peripheral collisions, to three IMF sources for more central ones. The source picture is very similar for the three different impact parameter filters.

In Fig. 3 the energy threshold limit (for $Z = 5$) is indicated by solid lines for AMPHORA with ionization chambers, and by dotted lines for standard AMPHORA without ionization chambers. As one can see, without ionization chambers the IMF source located at negative velocities could not be observed.

The sources at positive and negative velocities come from decays of the PLF and TLF (this was verified by simulation). Due to asymmetry of the AMPHORA filter the shape of PLF and TLF ''hills'' is different. The PLF ''hill'' has a larger base and is lower. The TLF one has a smaller base and is taller, as the TLF particles are seen only in the two detector rings equipped with ionization chambers. TLF's at smaller angles are not observed because of energy thresholds. For larger lab angles TLF's are not identified. Consequently, for the TLF source we observe only larger transverse velocities.

The explanation for the mid velocity source is less obvious. For example it could be produced as a superposition from decays of the PLF and TLF. To investigate this possibility we display in Fig. 4 distributions of events in the GI velocity plot for IMF's (events with 3 IMF's) with border lines (somewhat arbitrary) separating the three source regions. These borders are shown as solid lines. No impact parameter filters were applied. In Fig. 4 predictions of an event generator are also presented. Event generator simulates the composite system formation and decay at L values small enough, the DIC scenario at properly large L values and has no subroutine to produce IMF's from the intermediate velocity source [14,17]. Figures 4(a) and 4(b) was prepared under

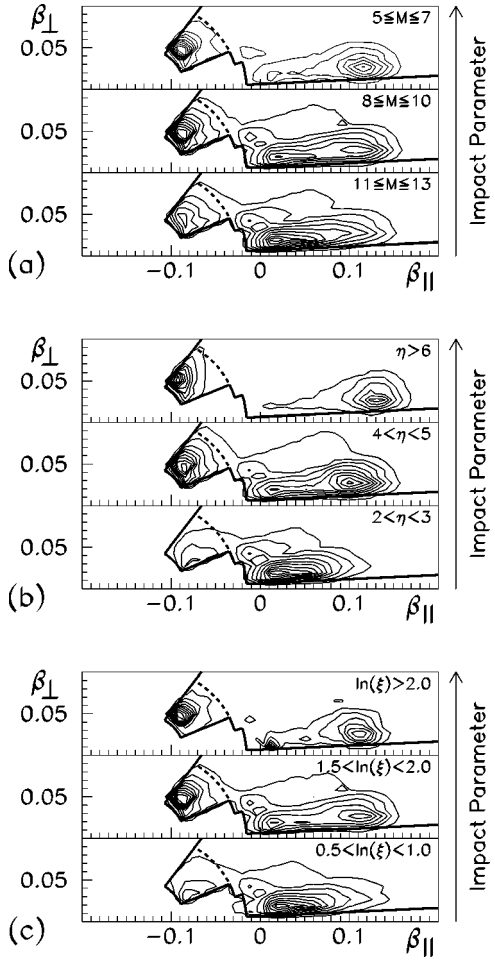

FIG. 3. GI velocity ($\beta = v/c$) plots of IMF's for different bins of M (a), η (b), and ξ (c), serving as impact parameter filters. Events with $m = 3$. Solid and dotted lines indicate energy thresholds ($Z = 5$) for the case with and without ionization chambers, respectively.

a condition that in each event at least one fragment exists in the IVS region. For clarity, the contour lines corresponding only to two other IMF's are presented. These two other IMF's can be located everywhere. As one can see, experiment reveals two sources (the third one in the middle exists, but is not presented), while the event generator creates a completely different picture. Figures 4(c) and 4(d) display a situation where in each event at least one IMF is located in the TLF region and one in the PLF region. Contour lines of the third IMF only are presented. As before all three sources exist in the experiment (two of them are not presented). The IVS is clearly observed in a similar location as in Fig. 3. Again the event generator crates something very different. A maximum observed here is due to the PLF decay and corresponds to fragments located outside the arbitrarily assumed PLF region.

Evidence of Fig. 4 shows that the IVS can not be produced as a superposition from decays of the PLF and TLF. Therefore one can say that in Fig. 3 we see indeed an intermediate velocity source of particles. It is slightly shifted from the c.m. position towards higher velocities because of the AMPHORA forward-backward energy threshold asymmetry.

The IVS exists also in events with four and five IMF's. Its evolution with the impact parameter is presented in Fig. 5 for

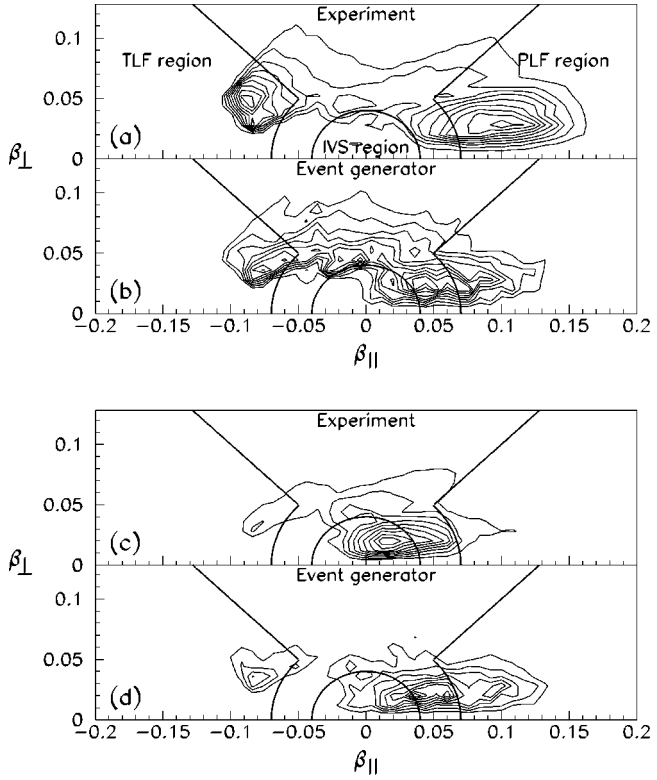

FIG. 4. Distribution of IMF's in the GI velocity ($\beta = v/c$) plot for events with $m = 3$ and in coincidence with IVS (a),(b), or with the PLF and TLF regions (c),(d). Solid lines separate the three source regions. Experimental data and event generator predictions are presented.

events with $m = 4$ (a), and $m = 5$ (b), respectively. The number of such events is much smaller compared with the $m = 3$ case, especially for peripheral collisions, where the PLF and TLF excitation energy is usually too small for emission of more than one IMF.

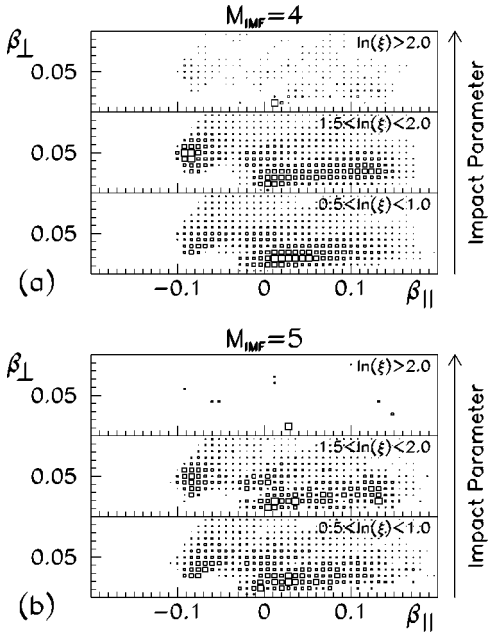

FIG. 5. GI velocity ($\beta = v/c$) plots of IMF's for different bins of ξ serving as impact parameter filter. Events with $m = 4$ (a) and $m = 5$ (b).

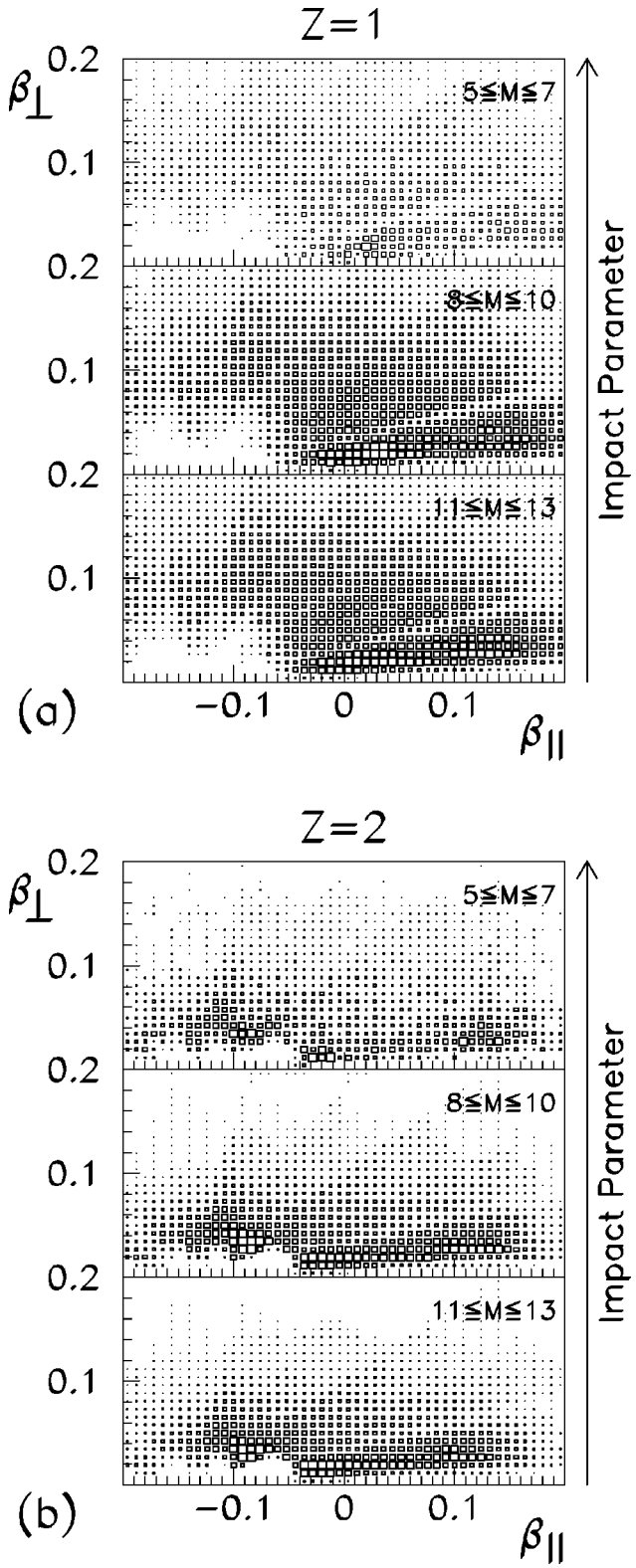

FIG. 6. GI velocity ($\beta = v/c$) plots of $Z=1$ (a) and $Z=2$ (b) particles, for different bins of M.

A systematic trend can be observed in the probability for events which include an intermediate velocity source. Thus an IVS can be found in 23, 29, and 34% of events having 3, 4, and 5 IMF's, respectively.

One may ask if an IVS can also be observed for light particles. Figures 6(a) and 6(b) present GI velocity distributions for $Z=1$ and $Z=2$ particles, respectively, in different bins of b, selected with the M filter. For protons no distinct sources are seen, probably because of multiple cascade emission and high proton velocities. For alphas three maxima can be observed, especially for $5<M<7$ and $8<M<10$. However, in this case it is not possible to exclude a possibility, that part of the source in the middle comes from a superposition from decays of the PLF and TLF.

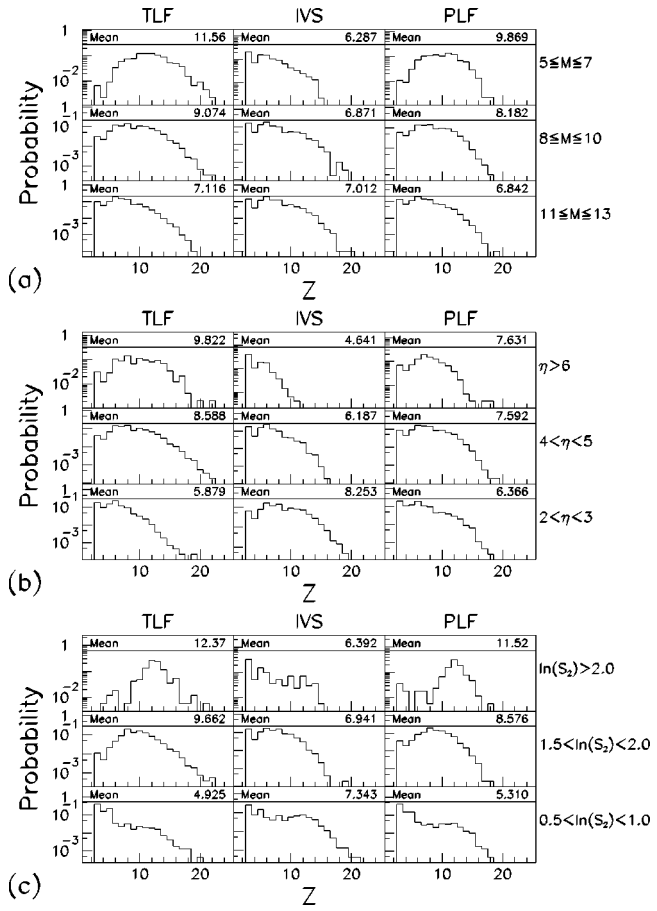

FIG. 7. Charge distributions of IMF's from the TLF, IVS, and PLF source, respectively, for different filter bins. Numbers indicate average charge values. Events with $m=3$.

D. Charge distributions

In order to investigate the distribution of charges between the three sources we use the border lines of Fig. 4 and a condition, that an IMF is observed in each source region.

Distribution of charges between the TLF, IVS, and PLF sources ($m=3$) is given in Fig. 7 and average fractions of charges from different sources are shown in Fig. 8, as a function of the impact parameter related variables. Direction of the increasing impact parameter is also indicated. As one can see, for $m=3$, the IMF charge is more concentrated in the PLF and TLF sources for more peripheral collisions, while the IVS becomes more important for more central collisions. A similar trend is observed for $m=4$. For $m=5$ it is less distinct.

E. Transition towards central collisions

Up to now our analysis of data was restricted to the region of midcentral collisions with impact parameters in the range

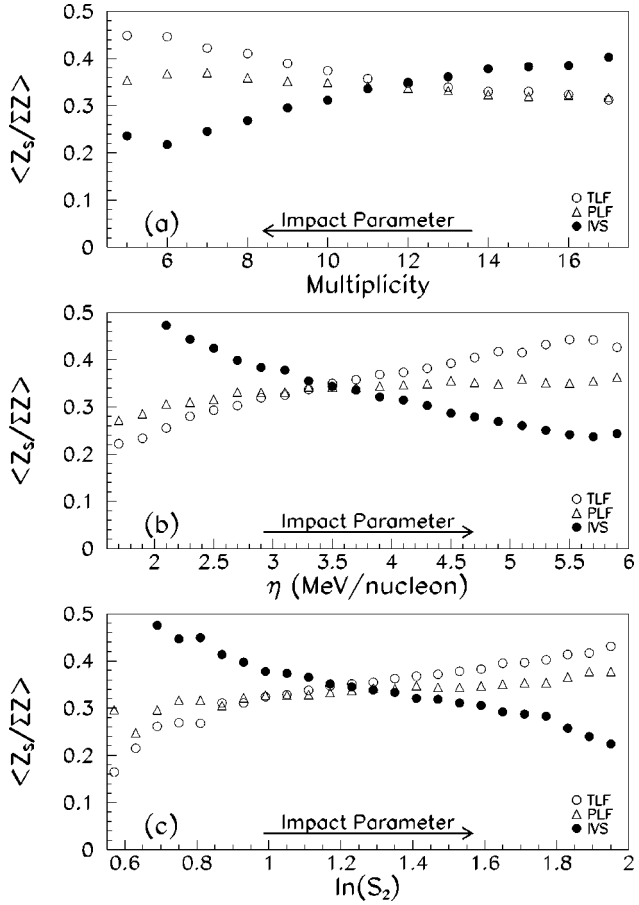

FIG. 8. Average fractions of the IMF charges in the TLF, IVS and PLF source, respectively, versus M (a), η (b), and lnS_2 (c). Events with $m=3$.

from about 4 to 6 fm. We now briefly investigate the evolution of the IMF sources for more central collisions. We shall use here a ρ filter, described in detail in Refs. [13] and [14]. We introduce a coordinate system x,y,z with $x=p_1/p_p, y=v_{\rm rel}/v_{pt}, z=\epsilon$. Here p_1, p_p, v_{pt}, and ϵ are the momentum of the heaviest fragment in an event, the projectile c.m. momentum, the entrance channel projectile-target relative velocity, and the event elongation ϵ in the momentum space, respectively. Relative velocity of the heaviest fragment detected in an event and of the second heaviest is denoted as $v_{\rm rel}$. We define the global variable ρ as

$$\rho=\sqrt{x^2+y^2+z^2}. \tag{3}$$

Each event is represented now by a point in the x,y,z space. Its dimensionless coordinates x,y,z have values from 0 to 1. It is clear, that for nearly central collisions events should be located close to the origin of the coordinate system (small ρ values). For DIC's and quasielastic collisions one expects events up to $\rho=3^{1/3}$.

Figure 9 presents GI velocity plots for IMF's (events with three IMF's) for different ρ bins. We observe here evolution from three sources into practically one midvelocity source.

For sufficiently central collisions contribution of events having IMF's coming from the PLF and TLF source is very small. For $\rho<0.5$ it is 1, 2.8, and 8% for events with 3, 4, and 5 IMF's, respectively.

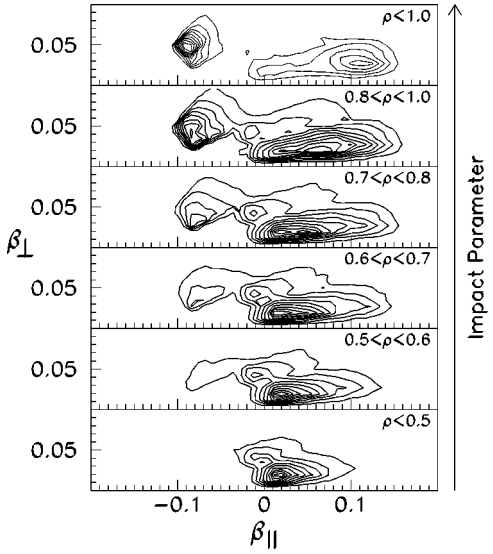

FIG. 9. GI velocity ($\beta=v/c$) plots of IMF's for different bins of ρ serving as impact parameter filters. Events with $m=3$.

III. BNV CALCULATIONS

We employ a standard BNV code [18]. It simulates evolution of the reaction dynamics solving the Boltzmann-Nordheim-Vlasov kinetic equation with a large number (40) of test particles per nucleon. Calculations were performed for local Skyrme forces corresponding to a soft equation of state ($K=200$ MeV). The calculations suggest intermediate values

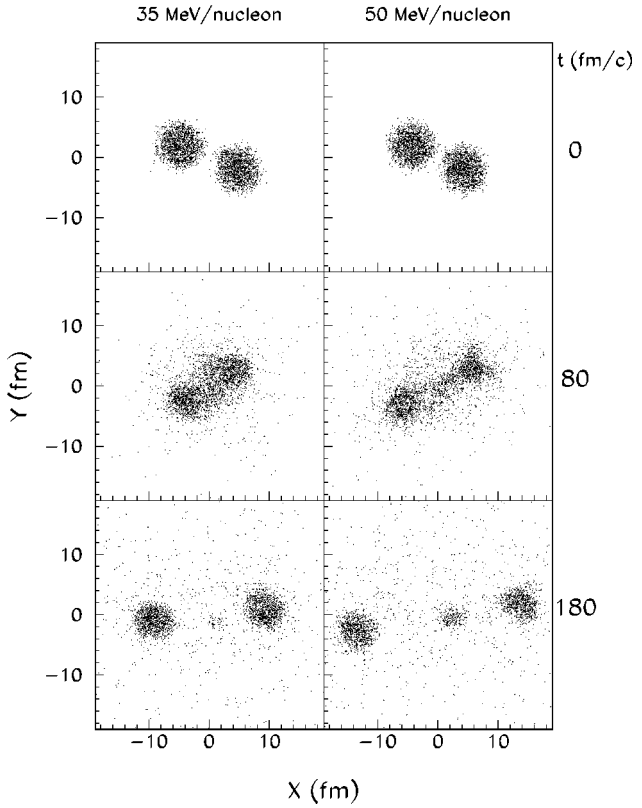

FIG. 10. Density scatter plots in the reaction plane obtained from BNV calculations for different moments of time (fm/c) and $b=4$ fm, $K=200$ MeV. ^{40}Ca+^{40}Ca reaction at $E_{\rm lab}=$ 35 and 50 MeV/nucleon.

of b as a region of impact parameters where the intermediate velocity source of IMF's is most likely to be produced.

Figure 10 presents density scatter plots in the reaction plane for different moments of time (fm/c) and impact parameter $b=4$ fm. The calculations were carried out for 35 MeV/nucleon and for 50 MeV/nucleon ^{40}Ca+^{40}Ca collisions. We clearly observe evolution of the ''neck'' region and disintegration of the system into three sources. Creation of the IVS is more distinctly observed at 50 MeV/nucleon.

For a hard equation of state, $K=380$ MeV, the ''neck'' formation and rupture are not seen in the BNV simulations.

One should cite here Landau-Vlasov calculations [19] made almost 10 years ago for the ^{40}Ca+^{40}Ca reaction and collision energies 20–100 MeV/nucleon. They suggested appearance of several sources for higher collision energies and larger impact parameters.

IV. SUMMARY AND DISCUSSION

In this work we have studied sources of intermediate mass fragments for the ^{40}Ca+^{40}Ca reaction at $E_{\rm lab}=35$ MeV/nucleon. The experimental data not only reveals the existence of PLF and TLF sources but also provides strong evidence for the existence of an intermediate velocity source. This latter source is already visible in the GI velocity plot but has been confirmed by more sophisticated gating techniques. The IVS is not observed in all events. This suggests a stochastic character of its creation. The number of events in which an IVS has been found increases from 23 to 34% with the number of IMF's increasing from 3 to 5, respectively.

It was shown in previous papers [13,14] that for sufficiently central ^{40}Ca+^{40}Ca collisions a composite system is formed. It is difficult to say if for more central collisions the IVS will evolve into a decaying composite system, formed in more or less incomplete fusion, or if both reaction scenarios are different and independent.

The calculations of the Boltzmann-Nordheim-Vlasov type suggest a creation of an intermediate velocity source in the ''neck'' region between colliding nuclei and for impact parameters corresponding to mid central collisions, but underestimate its ''strength'' at 35 MeV/nucleon. However, these calculations do not include two body and higher order correlations. This fact may be responsible for this distinct difference with experiment.

ACKNOWLEDGMENTS

The authors are indebted to Dr. Gordon J. Wozniak for supplying a working version of the BNV code. This work was supported by the Polish-French (IN_2P_3) agreement and the Committee of Scientific Research of Poland (KBN Grant No. PB719/P3/93/04).

[1] See, for example, W. U. Schröder and J. R. Huizenga, in *Treatise on Heavy-Ion Science*, edited by D. A. Bromley (Plenum, New York, 1984), Vol. 2, pp. 113–726.

[2] See W. U. Schröder, Nucl. Phys. **A538**, 439c (1992).

[3] J. Péter, S. C. Jeong, J. C. Angélique, G. Auger, G. Bizard, R. Brou, A. Buta, C. Cabot, Y. Cassagnou, E. Crema, D. Cussol, D. Durand, Y. El Masri, P. Eudes, Z. Y. He, A. Kerambrun, C. Lebrun, R. Legrain, J. R. Patry, A. Péghaire, R. Régimbart, E. Rosato, F. Saint-Laurent, J. C. Steckmeyer, B. Tamain, and E. Vient, Nucl. Phys. **A593**, 95 (1995).

[4] L. Stuttgé, J. C. Adloff, B. Bilwes, R. Bilwes, F. Cosmo, M. Glaser, G. Rudolf, F. Scheibilng, R. Bougault, J. Colin, F. Delaunay, A. Genoux-Lubain, D. Horn, C. Le Brun, J. F. Lecolley, M. Louvel, J. C. Steckmeyer, and J. L. Ferrero, Nucl. Phys. **A539**, 511 (1992); B. Lott, S. P. Baldwin, B. M. Szabo, B. M. Quednau, W. U. Schröder, J. Tõke, L. G. Sobotka, J. Barreto, R. J. Charity, L. Gallamore, D. G. Sarantites, D. W. Stracener, and R. T. De Souza, Phys. Rev. Lett. **68**, 3141 (1992); G. Cassini, P. G. Bizzeti, P. R. Maurenzig, A. Olmi, A. A. Stefanini, J. P. Wessels, R. J. Charity, R. Freifelder, A. Gobbi, N. Herrmann, K. D. Hildenbrand, and H. Stelzer, *ibid.* **71**, 2567 (1993); C. P. Montoya, W. G. Lynch, D. R. Bowman, G. F. Peaslee, N. Carlin, R. T. De Souza, C. K. Gelbke, W. G. Gong, Y. D. Kim, M. A. Lisa, L. Phair, M. B. Tsang, J. B. Webster, C. Williams, N. Colonna, K. Hanold, M. A. McMahan, G. J. Wozniak, and L. G. Moretto, *ibid.* **73**, 3070 (1994); J. Tõke, B. Lott, S. P. Baldwin, B. M. Quednau, W. U. Schröder, L. G. Sobotka, J. Barreto, R. J. Charity, D. G. Sarantites, W. Stracener, and R. T. De Souza, *ibid.* **75**, 2920 (1995).

[5] J. Tõke, B. Lott, S. P. Baldwin, B. M. Quednau, W. U. Schröder, L. G. Sobotka, J. Barreto, R. J. Charity, L. Gallamore, D. G. Sarantites, D. W. Stracener, and R. T. De Souza, Nucl. Phys. **A583**, 519 (1995).

[6] J. F. Dempsey, R. J. Charity, L. G. Sobotka, G. J. Kunde, S. Gaff, C. K. Gelbke, T. Glasmacher, M. J. Huang, R. C. Lemmon, W. G. Lynch, L. Manduci, L. Martin, M. B. Tsang, D. K. Agnihotri, B. Djerroud, W. U. Schröder, W. Skulski, J. Tõke, and W. A. Friedman, Phys. Rev. C **54**, 1710 (1996); Y. Larochelle, L. Gingras, L. Beaulieu, X. Quian, Z. Saddiki, B. Djerround, D. Doré, R. Laforest, R. Roy, M. Samri, C. St-Pierre, G. C. Ball, D. R. Bowman, A. Galindo-Uribarri, E. Hagberg, D. Horn, J. A. López, and T. Robinson, *ibid.* **55**, 1869 (1997); J. Łukasik, J. Benlliure, V. Métivier, E. Plagnol, B. Tamain, G. Auger, Ch. O. Bari, E. Bisquer, B. Borderie, R. Bougault, R. Brou, Ph. Buchet, J. L. Charvet, A. Chbihi, J. Colin, D. Cussol, R. Dayras, A. Demeyer, D. Doré, D. Durand, P. Eudes, E. Gerlic, D. Gourio, D. Guinet, P. Lautesse, J. L. Laville, J. F. Lecolley, A. Le Fèvre, T. Lefort, R. Legrain, O. Lopez, M. Louvel, N. Marie, L. Nalpas, M. Parlog, J. Péter, O. Politi, A. Rahmani, T. Reposeur, M. F. Rivet, E. Rosato, F. Saint-Laurent, M. Squalli, J. C. Steckmeyer, M. Stern, L. Tassan-Got, E. Vient, C. Volant, J. P. Wieleczko, M. Colonna, F. Haddad, Ph. Eudes, T. Sami, and F. Sebille, *ibid.* **55**, 1906 (1997).

[7] L. G. Sobotka, Phys. Rev. C **50**, R1272 (1994).

[8] M. Colonna, M. Di Toro, A. Guarnera, V. Latora, A. Smerzi, and Z. Jiquan, Nucl. Phys. **A583**, 525 (1995).

[9] U. Brosa, S. Grossmann, and A. Müller, Phys. Rep. **197**, 167 (1990).

[10] See J. P. Theobald, P. Heeg, and M. Mutter, Nucl. Phys. **A502**, 343c (1989).

[11] D. Drain, A. Giorni, D. Hilscher, C. Ristori, J. Alaria, G. Barbier, R. Bertholet, R. Billerey, B. Chambon, B. Cheynis, J. Crancon, A. Dauchy, P. Désesquelles, A. Fontenille, L. Guyon, D. Heuer, A. Lléres, M. Maurel, E. Monnand, C. Morand, H. Nifenecker, C. Pastor, J. Pouxe, H. Rossner, J. Saint-Martin, F. Schussler, P. Stassi, M. Tournier, and J. B. Viano, Nucl. Instrum. Methods Phys. Res. A **281**, 528 (1989).

[12] T. Barczyk, J. Brzychczyk, P. Burzyński, W. Gawlikowicz, K. Grotowski, S. Micek, P. Pawłowski, R. Płaneta, A. J. Cole, A. Chabane, P. Désesquelle, A. Giorni, D. Heuer, A. Lléres, J. B. Viano, D. Benchekroun, B. Cheynis, A. Demeyer, E. Gerlic, D. Guinet, P. Lautesse, L. Lebreton, M. Stern, and L. Vagneron, Nucl. Instrum. Methods Phys. Res. A **364**, 311 (1995).

[13] P. Pawłowski, D. Benchekroun, E. Bisquer, J. Brzychczyk, P. Burzyński, A. Chabane, M. Charvet, B. Cheynis, A. J. Cole, A. Demeyer, P. Désesquelles, W. Gawlikowicz, E. Gerlic, A. Giorni, K. Grotowski, D. Guinet, P. Hachaj, D. Heuer, P. Lautesse, L. Lebreton, A. Lléres, S. Micek, R. Płaneta, Z. Sosin, M. Stern, L. Vagneron, J. B. Viano, and A. Wieloch, Phys. Rev. C **54**, R10 (1996).

[14] P. Pawłowski, D. Benchekroun, E. Bisquer, J. Brzychczyk, A. Chabane, M. Charvet, B. Cheynis, A. J. Cole, A. Demeyer, P. Désesquelles, W. Gawlikowicz, E. Gerlic, A. Giorni, K. Grotowski, D. Guinet, P. Hachaj, D. Heuer, P. Lautesse, L. Lebreton, A. Lléres, S. Micek, R. Płaneta, Z. Sosin, M. Stern, L. Vagneron, J. B. Viano, and A. Wieloch, Z. Phys. A **357**, 387 (1997).

[15] X. Campi, J. Phys. A **19**, L917 (1986).

[16] M. Belkacem, P. F. Mastinu, V. Latora, A. Bonasera, M. D'Agostino, M. Bruno, J. D. Dinius, M. L. Fiandri, F. Gramegna, D. O. Handzy, W. C. Hsi, M. Huang, G. F. Margagliotti, P. M. Milazzo, C. P. Montoya, G. F. Peaslee, R. Rui, C. Schwarz, G. Vannini, and C. Williams, Phys. Rev. C **54**, 2435 (1996).

[17] Z. Sosin, K. Grotowski, A. Wieloch, and H. W. Wilschut, Acta Phys. Pol. B **25**, 1601 (1994); Z. Sosin, J. Brzychczyk, K. Grotowski, J. D. Hinnefeld, E. E. Koldenhof, H. K. W. Leegte, J. Łukasik, S. Micek, R. Płaneta, R. H. Siemssen, A. Wieloch, and H. W. Wilschut, Nucl. Phys. **A574**, 474 (1994).

[18] A. Bonasera, G. Russo, and H. H. Woler, Phys. Lett. B **246**, 337 (1990).

[19] K. Sneppen and L. Vinet, Nucl. Phys. **A480**, 342 (1988).